Impact of magnetic perturbations on the divertor heat load in L- and H-Mode at ASDEX Upgrade

M. Faitsch, B. Sieglin, T. Eich, A. Herrmann, W. Suttrop and the ASDEX Upgrade Team

Max-Planck-Institute for Plasma Physics, Boltzmannstr. 2, D-85748 Garching, Germany

Introduction

The control of transient heat loads induced by edge localised modes (ELM) in H-Mode is essential to the success of ITER/DEMO. The application of 3D magnetic perturbation (MP) fields is studied as a method for ELM control. However, these 3D fields lead to toroidal asymmetries of the heat load pattern at the divertor target that may be problematic for future devices [1]. ASDEX Upgrade is equipped with a versatile set of magnetic perturbation coils [2] and a high resolution infrared (IR) camera system [3] to characterise the impact of MPs on divertor heat loads in both L- and H-Mode. The MP field can be rotated toroidally by altering the currents inside the MP coils in order to access the full 2D profiles. In this paper we present results in ASDEX Upgrade L-Mode experiments [4, 5] and compare them to H-Mode inter-ELM heat flux profiles. Additionally, the influence of MP on the ELM filament heat deposition location is discussed.

Discharge parameters

The discharges discussed in this paper have a toroidal field strength of -2.5 T and a plasma current of 0.8 MA. The applied current in the MP coils is 1 kA with a phasing between the two rows of -90 degree. This is the resonant configuration for field lines at the plasma edge (q = 5) for the vacuum field approximation. The currents are altered in order to rigidly rotate the MP field with 1 Hz. The H-Mode (#33222) has the same plasma shape and applied MP as the L-Mode (#32217), with the only changes being the electron cyclotron heating power (2.7 MW (H-Mode) compared to 0.37 MW (L-Mode)) and the density (line averaged edge density: $3.3 \cdot 10^{19}\text{m}^{-3}$ (H-Mode) compared to $0.8 \cdot 10^{19}\text{m}^{-3}$ (L-Mode)). The MP in the presented H-Mode has a moderate effect on density and ELM frequency, which assures long enough inter-ELM periods for stable divertor conditions.

The resulting 2D heat flux structure in L-Mode and inter-ELM H-Mode are compared to an ad-hoc model presented in [5]. This model uses field line tracing starting at the outer divertor target up to the outer mid plane (OMP). The magnetic field used is the axisymmetric equilibrium field superimposed with the magnetic field induced by the currents inside the MP coils. No plasma response is taken into account, therefore this is called the vacuum field approximation. Every field line is associated with heat flux assuming an exponentially decaying profile at the OMP starting from a corrugated separatrix. The decay length is chosen to be the power fall-off length λ_q obtained from a reference time window without MP within the same discharge. A Gaussian is convoluted at the target, with the width S being the divertor broadening from the axisymmetric reference.

L-Mode

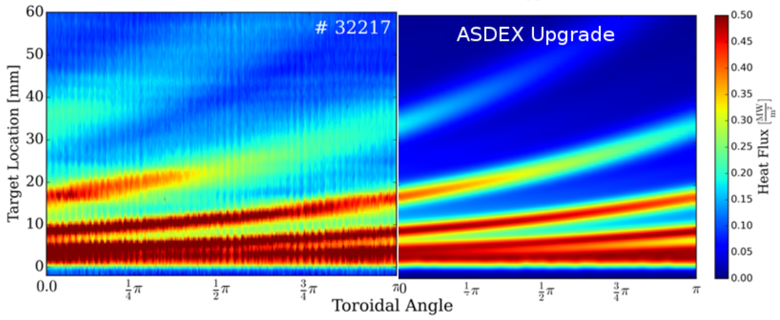

Figure 1: Comparison of the 2D heat flux pattern for L-Mode between measured heat flux from IR thermography (left) and modelled heat flux (right) [5].

L-Mode experiments offer the possibility to have stable divertor and plasma conditions. This is ideal to investigate in detail the effect of MPs on the heat flux profile with a rigidly rotated MP field.

At low density a pronounced 2D heat flux structure is observed with resonant MP. This structure is reproduced by the ad-hoc model [5]. A comparison between the experimental measurement (left) and modelled heat load pattern (right) is shown in Fig. 1. In Fig. 2 a target heat flux profile in the reference phase without MP (blue) is compared to a profile with MP (red) and a toroidally averaged profile with MP (black). The averaged profile with MP is described by the same two transport qualifiers λ_q and S as the reference heat flux profile. The values for both transport qualifiers are the same comparing the reference (W/O MP) to the averaged profile (With MP).

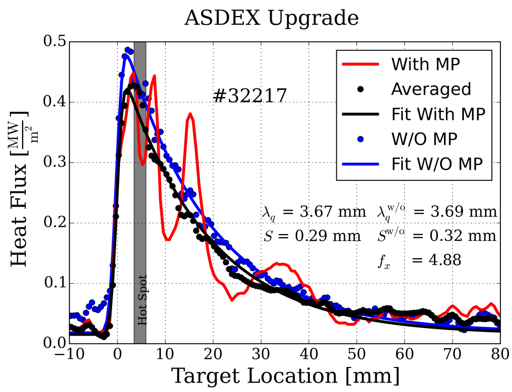

Figure 2: L-Mode heat flux profiles with MP (red), without MP (blue) and averaged over a full toroidal period of the MP (black) measured with IR thermography [5].

With increasing divertor broadening S the 2D characteristic becomes less pronounced [4], leading to nearly toroidally symmetric profiles at moderate values of $S/\lambda_q > 0.5$ in L-Mode.

H-Mode: inter-ELM

In H-Mode plasmas the heat flux is divided into two periods, the heat flux associated with ELM crashes and the inter-ELM, *steady state*, heat flux.

The inter-ELM heat flux without MP is characterised with the same transport model as the L-Mode heat flux profile. In H-Mode significantly more power is deposited at the divertor target and an in general smaller λ_q is observed.

In Fig. 3 a comparison between the inter-ELM heat flux pattern from experimental measurements (left) and modelling (right) is shown. The presented inter-ELM heat flux consists of time slices, averaged in the period between 70-90% between consecutive ELMs and normalised to the deposited power.

The heat flux extend along the target location is reduced compared to the L-Mode due to a narrower power fall-off length λ_q, which is reproduced in the modelled heat flux.

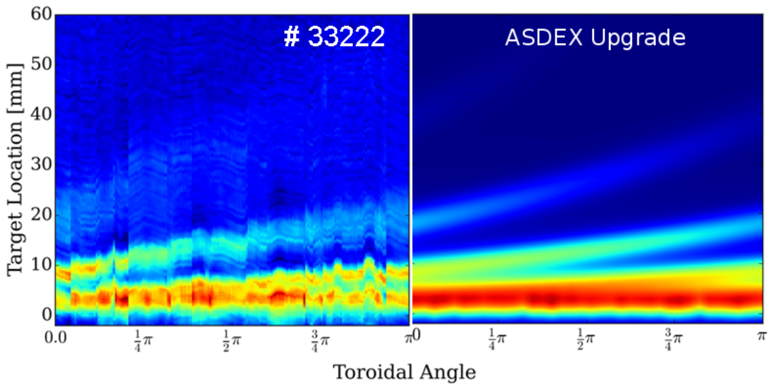

Figure 3: Comparison of the 2D heat flux pattern for inter-ELM H-Mode between the measured heat flux from IR thermography (left) and modelled heat flux (right).

H-Mode: ELMs

Large ELMs in future devices might limit the life-time of plasma facing components. The control or possible suppression of them is therefore mandatory.

A recent scaling was established for ASDEX Upgrade, JET and MAST for the ELM peak energy fluence [6] with the main parameter being the pressure at the top of the pedestal. Type-I ELMs during phases with MP follow this scaling at ASDEX Upgrade [7].

In this paper the effect of the MP on the ELM filaments location is shown. ELM filaments, without MP being expelled at random positions, may *lock* to the external MP field [8]. In Fig. 4 the time trace of heat flux at the outer divertor target measured with IR thermography is shown.

The phase with MP (3.0 - 6.0 s) is marked with vertical white lines. The ELM filament position for the individual ELMs is depicted with white dots. Before and after the phase with MP the position is stochastic. During the MP phase the position of the filaments coincides with the position of elevated inter-ELM heat flux.

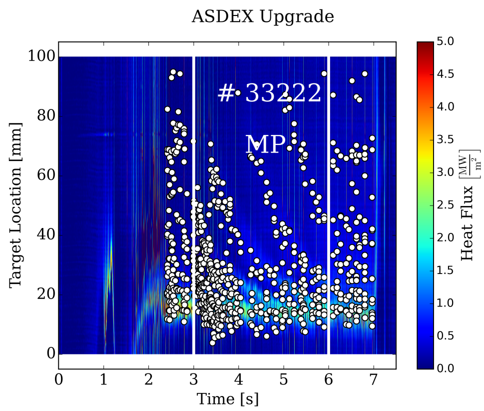

Figure 4: H-Mode heat flux time trace with superimposed ELM filament location (white dots). The phase with MP is between 3.0-6.0 s (white vertical lines).

Conclusions

Applying external MP leads to a change in the divertor heat flux pattern. The inter-ELM and L-Mode profile, being axisymmetric without MP, develops a 2D structure. This structure is in agreement with a vacuum field line tracing model for the presented discharges in both L- and H-Mode. The toroidally averaged heat flux profile with MP is similar to the reference profile without MP, being characterised by the same transport qualifiers, power fall-off length λ_q and divertor broadening S. ELM filaments, without MP being expelled at random positions, may *lock* to the external MP field, possibly leading to enhanced sputtering and thermal loads on distinguished toroidal locations with respect to the phase of the MP.

Acknowledgements

This work has been carried out within the framework of the EUROfusion Consortium and has received funding from the Euratom research and training programme 2014-2018 under grant agreement No 633053. The views and opinions expressed herein do not necessarily reflect those of the European Commission.

References

[1] A. Loarte, G. Huijsmans, S. Futatani et al., Nuclear Fusion (2014)
[2] W. Suttrop, O. Gruber, S. Günter et al., Fusion Engineering and Design (2009)
[3] B. Sieglin, M. Faitsch, A. Herrmann et al., Review of Scientific Instruments (2015)
[4] M. Faitsch, B. Sieglin, T. Eich et al., Nuclear Materials and Energy (2017)
[5] M. Faitsch, B. Sieglin, T. Eich et al., Plasma Physics and Controlled Fusion (2017)
[6] T. Eich, B. Sieglin, A. Thornton et al., Nuclear Materials and Energy (2017)
[7] B. Sieglin, T. Eich, M. Faitsch et al., Nuclear Fusion (2017)
[8] M. Jakubowski, T. Evans, M. Fenstermacher et al, Nuclear Fusion (2009)